



CANCOM2024 – CANADIAN INTERNATIONAL CONFERENCE ON COMPOSITE MATERIALS  
**MODELING HYPERVELOCITY IMPACTS ON CFRP COMPOSITES  
USING AN ADAPTIVE FEM-SPH METHOD**

Gudisey, Anthony<sup>1\*</sup> and Cherniaev, Aleksandr<sup>2</sup>

<sup>1</sup> Mechanical, Automotive and Materials Engineering, Ph.D Candidate, Windsor, ON, CA

<sup>2</sup> Mechanical, Automotive and Materials Engineering, Associate Professor, Windsor, ON, CA

\* Corresponding author (gudisey@uwindsor.ca)

**Keywords:** *Hypervelocity Impact, Adaptive modelling, Delamination*

## **ABSTRACT**

Micro-meteorites and orbital debris (MMOD) pose a prevalent threat to the operational integrity of satellites through hypervelocity impacts (HVI), at or exceeding speeds of 7 km/s. These events can cause damage to the satellite equipment and the associated consequences can be measured through loss of operation and the corresponding economic impacts for replacement. Due to the high economic expenses associated with physical testing, numerical modeling of HVI on space structures is widely used in their design. The increasing use of advanced composites in space applications, such as carbon fiber reinforced polymers (CFRPs), requires the development of numerical models capable of predicting composites' damage and failure under such extreme loading conditions. Numerical techniques traditionally employed in HVI problems include the Lagrangian implementation of the finite element method (FEM; excellent for tracking the relative motion between interfaces, e.g. in modeling delamination) and the meshfree smoothed particles hydrodynamics technique (SPH; great at replicating extreme deformation and fragmentation). In this study, the adaptive FEM-SPH method was employed to exploit the benefits of both techniques simultaneously. The laminated composites are studied under impact by projectiles of different materials (steel, aluminum, and nylon), replicating different types of orbital debris according to NASA classification (high, medium, and low-density debris). The results of simulations are compared against available experimental data.

## **1 INTRODUCTION**

Composite materials, especially CFRPs, are extensively used in satellite structures. The operational and structural safety of satellites is hindered by HVIs with micro-meteoritic materials travelling at speeds in excess of 7 km/s [1]. Shielding is used in satellites as a preliminary line of defense to dissipate energy and break up the incoming projectile, protecting the operational components of the spacecraft. The high impact velocities produce extremely large deformations and fragmentation, even when the projectiles are millimeter sized. While experimental test setups exist to replicate these impacts, the economic cost associated with these tests is usually very high [2]. In addition, conducting a plethora of tests, with varying projectile densities, sizes and incident impact angles, is a taxing task.

Throughout the literature, there are many experimental studies exploring projectile impacts exceeding 3 km/s on facesheet materials. However, far fewer experimental studies exist exploring impacts at or close to the 7 km/s HVI range on CFRP facesheets. Rice University, University of Kent at Canterbury (UKC), Johnson Space Center (JSC) and Southwest Research Institute (SwRI), have conducted experiments on CFRP facesheets, mostly at the sub 7 km/s impact velocities, with a handful of experiments exceeding this threshold [3,4].

## CANCOM2024 – CANADIAN INTERNATIONAL CONFERENCE ON COMPOSITE MATERIALS

As an alternative to expensive physical testing, high quality numerical models, once extensively validated, can be used to simulate MMOD impacts. Traditional numerical models for HVI usually rely on either the Lagrangian implementation of the finite element method (FEM) with element erosion or use smoothed particle hydrodynamics (SPH) [5]. While the FEM is excellent for tracking the relative motion at interfaces caused by failure mechanisms, i.e., delamination, the process of element erosion is also subject to hourglassing, extreme element distortion and negative volume errors, all of which can cause low quality results in a simulation and non-physical failure characteristics. This is especially detrimental in HVI conditions where extreme deformation and material fragmentation are expressly present. As a result, the SPH method is usually preferred in these situations. This method provides high quality predictions in impact events where fragmentation is present. The SPH method, however, is incapable of modelling the cohesive interfaces between the ply layers and delamination in composites. This study proposes the use of a hybridized FEM to SPH modelling procedure to leverage the benefits of both modelling techniques and more comprehensively replicate the complete scope of failure mechanisms which will simultaneously occur and interact. Upon sufficient element distortion, the solid elements from the traditional FEM will erode and convert to SPH particles which retain the integrated properties of the solid elements which they replace. These SPH particles will be coupled to the adjacent solid elements, maintaining continuity so that minor deformations, further away from the highly localized fracture zone can be captured. There are three main objectives to this study:

- Numerically model the HVIs with the adaptive FEM to SPH method.
- Numerically model three different projectile densities with similar impact velocities.
- Perform sensitivity study to determine optimal erosion parameters for accurate crater size prediction.

## 2 Numerical Modelling

This study will focus on the numerical modelling of three physical experiments conducted by Rice University [3,4] on 16-ply AS4/PEEK (APC-2) composites, with a  $[0^\circ, 45^\circ, -45^\circ, 90^\circ]_{2s}$  orientation. The experiments labelled Rice #61, Rice #62 and Rice #63, will be abbreviated as R61, R62 and R63, respectively through the remainder of this manuscript. The projectiles explored within this study all possessed the same diameter but consisted of varying densities, to diversify the range of this study. The details pertaining to the projectiles are outlined as follows:

- R61 – 1 mm 440C Stainless Steel projectile, impacting at 7060 m/s – 1.84 mm thick facesheet
- R62 – 1 mm Aluminum 2017-T4 projectile, impacting at 7140 m/s – 1.84 mm thick facesheet
- R63 – 1mm Nylon projectile impacting at 6950 m/s – 1.73 mm thick facesheet

All the HVI shots were fired at  $0^\circ$  incidence angles, w.r.t the target. The models were created and run with LS-DYNA, single-precision MPP solver (R. 14.1).

### 2.1 Model Set-Up

The simulations each comprised of four parts, as shown in Figure 1a. The projectile (labelled 1) was created from only SPH particles as it was guaranteed to fragment during the impact process. The projectile was created from SPH particles that were 0.1 mm in size. The facesheet (labelled 2) was initially created with solid elements, and characteristic element lengths of 0.1 mm, to correspond to the projectile. The witness plate (labelled 3) whose purpose was to capture any debris from fragmentation and act as a second layer of protection, was modelled in the same way as the facesheet. Using the \*DEFINE\_ADAPTIVE\_SOLID\_TO\_SPH card, The solid facesheet and the witness plate were set to convert into SPH particles upon reaching sufficient erosion. A one-to-one adaptivity criterion was implemented to convert one solid element to one SPH particle, as shown in Figure 1b. Further, the SPH particle was

CANCOM2024 – CANADIAN INTERNATIONAL CONFERENCE ON COMPOSITE MATERIALS

coupled to the adjacent solid elements upon conversion. The SPH formulation 1 with re-normalization and solid element formulation 1 were used in all simulations. The \*SECTION\_SPH\_INTERACTION keyword was also used to prevent mixing of material properties between the facesheet and projectile. Finally, the non-reflecting boundary conditions (labelled 4) were implemented through the \*BOUNDARY\_NON\_REFLECTING and \*BOUNDARY\_SPH\_NON\_REFLECTING keywords to allow passage of stress waves.

**2.2 Material Modelling and Contact Algorithms**

Three different material models were used for the projectile, the facesheet and witness plate and the SPH variants of the facesheet and witness plate. Each of the projectiles was modelled through the Johnson-Cook (JC) material model (\*MAT\_015). The Mie-Gruneisen equation of state (EOS) was used to describe the volumetric expansion of the projectile due to the impact. The facesheet and witness plates were modelled with two different material models. The solid/SPH composite failure model (\*MAT\_059) with no EOS was primarily employed. Secondly, the composite damage material model (\*MAT\_022) with no EOS was employed as an alternative to \*MAT\_059. An add erosion (\*MAT\_ADD\_EROSION) was implemented with an effective strain-based failure criterion to control element deletion. Satisfying this failure criterion allowed the solid element to erode and become replaced by an SPH particle.

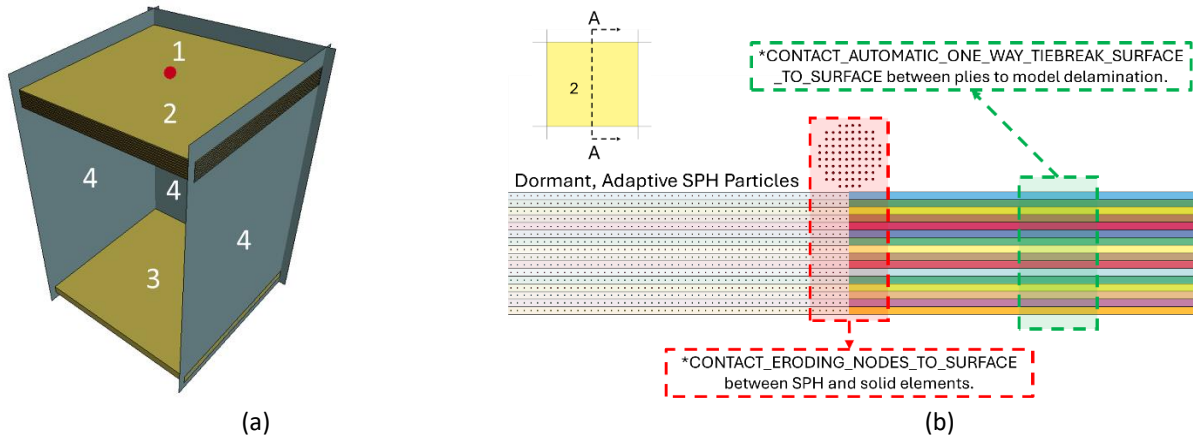


Figure 1: a) General schematic of the 16-ply laminate subject to HVI from micrometeorites and b) cross-sectional view of the laminate facesheet, with transparency turned on showing the dormant, adaptive SPH particles.

The contact algorithms within the simulations were set up in three steps. For contact between the SPH projectile, converted SPH facesheet and the solid elements in the facesheet, an eroding nodes to surface algorithm was invoked. Two part sets, one with the SPH parts and one with the solid parts were used to establish this contact. An eroding single surface algorithm was used for contact between adjacent, eroding solid ply layers, through part sets. Finally, an automatic one-way surface to surface tiebreak algorithm was invoked to model the adhesion between adjacent ply layers. Option 9 was used as it replicated the bilinear traction-separation law with zero thickness cohesive elements, similar to using a mixed mode cohesive material model (\*MAT\_138). Segment sets were used to establish this contact algorithm.

**3 Results and Discussions**

The predictions from the simulations were compared against the experimental observations and predictions from the empirically derived Tennyson equations [6], presented in [3,4], in the literature. The parameters used for validation include the crater size and the delamination area. The terms N, E and T refer to the numerical, experimental and Tennyson results, respectively. The columns labelled %, represent the relative error. The

CANCOM2024 – CANADIAN INTERNATIONAL CONFERENCE ON COMPOSITE MATERIALS

experiments presented in the literature presented two crater sizes, one for the entry crater and one for the exit, in this study, the equivalent crater area was computed through a top down view of the defeated CFRP facesheet, with ImageJ, from this area, an equivalent diameter value was computed. The equivalent diameter was then compared to the average of the two crater diameters presented in the literature. In all cases, the projectile perforated through the face sheet, and the corresponding debris cloud can be observed in Figure 2.

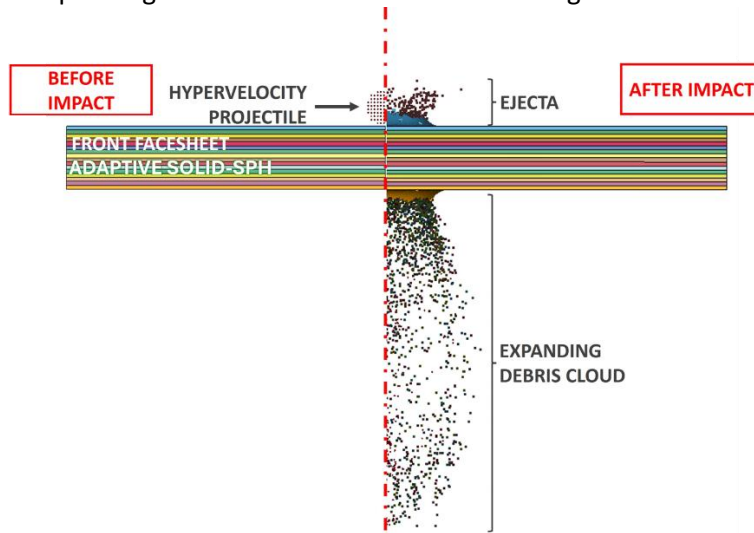


Figure 2: Debris cloud evolution in adaptive numerical model.

A sensitivity study was conducted to determine the erosion strain value (a non-physical parameter that requires careful calibration) that yielded the most accurate crater prediction. Figure 3 illustrates the variation of the crater size as a function of erosion strain. Table 1 provides a summary of the simulation results, with the respective relative errors computed at the best erosion criterion.

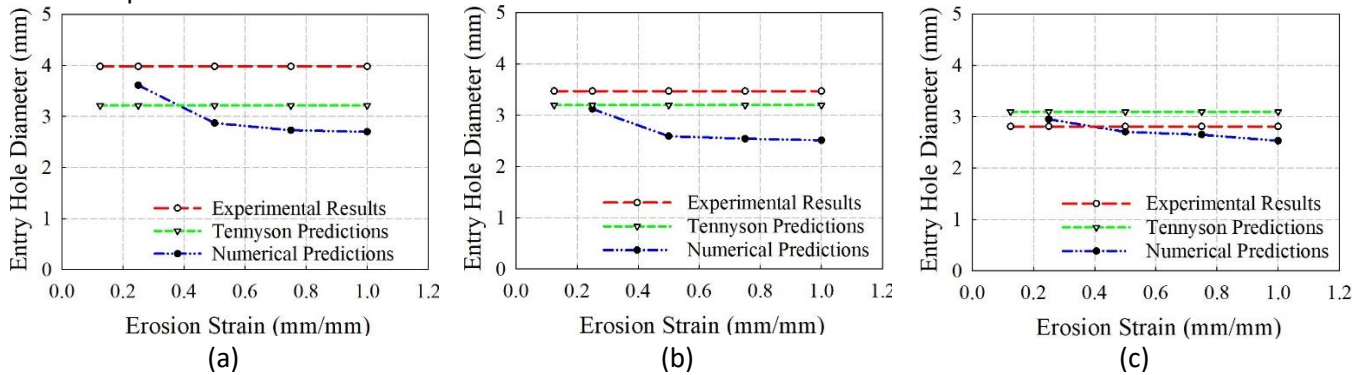


Figure 3: Crater prediction sensitivity to varied erosion strains in a) R61 (steel projectile), b) R62 (aluminum projectile) and c) R63 (nylon projectile).

Table 1: Summary of results from HVI simulations for steel (R61), aluminum (R62) and nylon (R63) projectiles.

Test	Impact speed (m/s)	Crater Diameter		Crater Diameter [3] (mm)	Crater Diameter	
		(mm)	(mm)		(mm)	(mm)
		N	E	%	T	%
R61	7060	3.61	3.27	10.08	3.21	2.92
R62	7140	3.12	3.62	9.30	3.19	12.97
R63	6950	2.95	2.83	4.98	3.09	4.77

### CANCOM2024 – CANADIAN INTERNATIONAL CONFERENCE ON COMPOSITE MATERIALS

The erosion strain values explored in this study were 0.125, 0.25, 0.50, 0.75 and 1.0 mm/mm. The general idea was that lower erosion strains would yield simulations with the lowest element distortion and hourglassing. The erosion strain criterion of 0.125 mm/mm caused excessive element deletion, especially away from the localized impact region. This occurred consistently between the three different projectile densities and as this was an undesirable result, it was excluded from every subsequent simulation. The lowest relative error between the predicted crater sizes and the ones determined from experiments corresponded with the 0.25 mm/mm erosion strain. The lowest relative errors were 10.08%, 9.30% and 4.98%, for R61, R62 and R63, respectively.

Delamination was another key outcome for this modelling procedure, however \*MAT\_059 was very stiff and delamination was not accurately predicted. The total values for delaminated area were presented in the experiments [3]. The \*EXTENT\_INTFOR and \*BINARY\_INTFOR keywords were used to measure delamination through the contact gap parameter. This parameter ranged from 0 to 1, where 0 represented no damage and 1 represented total separation. The images in Figure 4 illustrate a top down view through the laminates with transparency on so that delamination at each ply layer is shown, the highlighted regions indicate fully separated regions. Figure 4a presents the delamination as captured by \*MAT\_059, with the highlighted areas representing total separation. In comparison, Figure 4b exhibits the delamination captured by \*MAT\_022. It is immediately evident that the delamination is more pronounced and accurate when compared against experimental observations. Relative errors as low as 11.41% were noted with \*MAT\_022. The observed delamination patterns correspond with experimental and numerical observations [7]. The longitudinal stress waves travel along the direction of the fiber, and once the interply shear stresses become sufficiently high, cause cohesive failure in these directions. Converse to the crater size predictions, higher erosion strains were associated with better delamination predictions. Further, \*MAT\_022 proved to have a more difficult time while predicting crater size. Relative errors in crater prediction were only determined for R61, where relative errors ranged from 31.51% up to 43% for the 0.25 mm/mm and 1.0 mm/mm erosion strains, respectively.

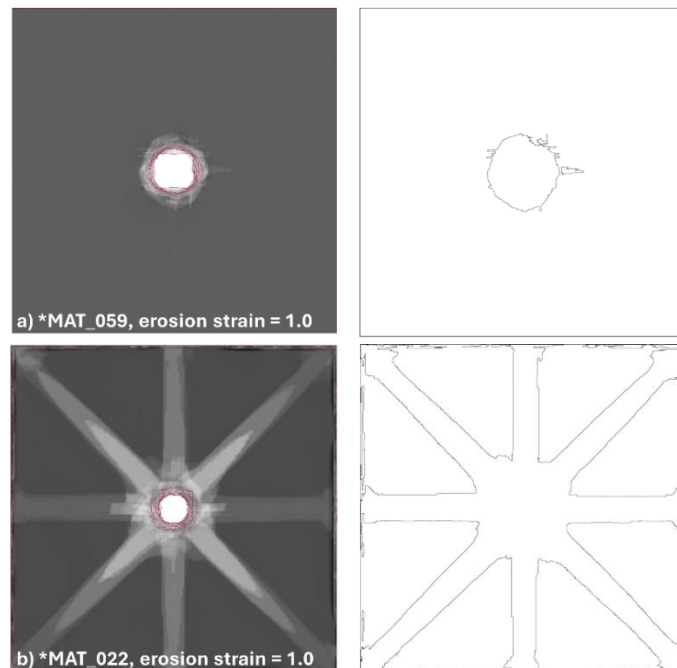


Figure 4: General top-down view of the delamination pattern observed through the laminate for a) \*MAT\_059 and b) \*MAT\_022.

## 4 Conclusions

The impetus of this study was to determine the capabilities of the adaptive FEM-SPH technique in modelling HVI scenarios. The advantages of each method could be leveraged, while minimizing their shortcomings. This could provide far more comprehensive damage prediction by capturing more failure modes than each method individually. Experiments conducted by Rice University [3] and empirically derived Tennyson equations [8] were used as a basis for comparing predictions from the simulations. Three projectile densities were modelled under HVIs of similar velocities. The key findings of this study are summarized as follows:

- A sensitivity study was conducted with \*MAT\_059 to study the effect of erosion strain on crater size. Findings indicated that lower erosion strains provided better prediction accuracy, with 0.25 mm/mm yielding the lowest relative error, when compared to experimental observations.
- The lowest observed errors were 10.08% for R61 (steel projectile), 9.30% for R62 (aluminum projectile) and 4.98% for R63 (nylon projectile).
- \*MAT\_059 was not capable of predicting delamination between plies with accuracy as it acted too stiff.
- \*MAT\_022 was used as an alternate material model to predict the delamination between plies. It was far more reliable in predicting delamination and as a general trend, it was noted that higher erosion strains led to higher delaminated area predictions, converse to the crater size observations. At an erosion strain of 0.75 mm/mm, relative errors of 11.41% were observed.
- \*MAT\_022 fell short in terms of predicting crater size, relative errors as high as 43% were observed.
- This study highlighted the adaptive FEM-SPH method's capabilities to provide more comprehensive damage modelling.
- Future steps include conducting sensitivity studies to enhance the crater size prediction capabilities of \*MAT\_022 and determining a middle ground for accurate crater size prediction and delaminated area.

## 5 References

- [1] S. K. Roy, M. Trabia, B. O'Toole, R. Hixson, S. Becker, M. Pena, R. Jennings, D. Somasoundaram, M. Matthes, E. Daykin and E. Machorro. "Study of hypervelocity projectile impact on thick metal plates". *Shock and Vibration*, Vol. 2016, Article ID 4313480, 2016.
- [2] M. J. Burchell, M. J. Cole, J. A. M. McDonnell and J. C. Zarnecki. "Hypervelocity Impact Studies using the 2MV Van de Graff Accelerator and Two-Stage Light Gas Gun of the University of Kent at Caterbury". *Measurement Science and Technology*, Vol. 10, pp. 41-50, 1999.
- [3] C. G. Lamontagne, G. N. Manuelpillai, J. H. Kerr, E. A. Taylor, R. C. Tennyson and M. J. Burchell. "Projectile Density, Impact Angle and Energy Effects on Hypervelocity Impact Damage to Carbon Fibre/PEEK Composites". *International Journal of Impact Engineering*, Vol. 26, pp. 381-398, 2001.
- [4] S. Ryan, M. Wicklein, A. Mouritz, W. Reidel, F. Schafer and K. Thoma. "Theoretical Prediction of Dynamic Composite Material Properties for Hypervelocity Impact Simulation". *International Journal of Impact Engineering*, Vol. 36, pp. 899-912, 2009.
- [5] A. Cherniaev. "Modelling of hypervelocity impact on open cell foam core sandwich panels". *International Journal of Impact Engineering*, Vol. 155, 103901, 2021.
- [6] R.C. Tennyson and C. Lamontagne. "Hypervelocity impact damage to composites". *Composites part A*, Vol. 31, pp 785-794, 2000.
- [7] A. Cherniaev and I. Telichev. "Numerical simulation of impact damage induced by orbital debris on shielded wall of composite overwrapped pressure vessel". *Applied Composite Materials*, Vol. 21, pp 861-884 2014.